Published in final edited form as:
J Neurophysiol. 2007 May ; 97(5): 3386–3395. doi:10.1152/jn.01270.2006.

Modulation of Inhibitory Activity by Nitric Oxide in the Thalamus

Sunggu Yang and **Charles L. Cox**
Department of Molecular and Integrative Physiology; Department of Pharmacology, College of Medicine; and Beckman Institute, University of Illinois, Urbana-Champaign, Urbana, Illinois

Abstract

The dorsal lateral geniculate nucleus (dLGN) is essential for the transfer of visual information from the retina to visual cortex, and inhibitory mechanisms can play a critical in regulating such information transfer. Nitric oxide (NO) is an atypical neuromodulator that is released in gaseous form and can alter neural activity without direct synaptic connections. Nitric oxide synthase (NOS), an essential enzyme for NO production, is localized in thalamic inhibitory neurons and cholinergic brain stem neurons that innervate the thalamus, although NO-mediated effects on thalamic inhibitory activity remain unknown. We investigated NO effects on inhibitory activity in dLGN using an in vitro slice preparation. The NO donor, SNAP, selectively potentiated the frequency, but not amplitude, of spontaneous inhibitory postsynaptic currents (sIPSCs) in thalamocortical relay neurons. This increase also persisted in tetrodotoxin (TTX), consistent with an increase in GABA release from presynaptic terminals. The SNAP-mediated actions were attenuated not only by the NO scavenger carboxy-PTIO but also by the guanylyl cyclase inhibitor ODQ. The endogenous NO precursor L-arginine produced actions similar to those of SNAP on sIPSC activity and these L-arginine–mediated actions were attenuated by the NOS inhibitor L-NMMA acetate. The SNAP-mediated increase in sIPSC activity was observed in both dLGN and ventrobasal thalamic nucleus (VB) neurons. Considering the lack of interneurons in rodent VB, the NO-mediated actions likely involve an increase in the output of axon terminals of thalamic reticular nucleus neurons. Our results indicate that NO upregulates thalamic inhibitory activity and thus these actions likely influence sensory information transfer through thalamocortical circuits.

INTRODUCTION

Visual information is transferred from the retina to the visual cortex by the dorsal lateral geniculate nucleus (dLGN) of thalamus. This information transfer is a dynamic process that can be strongly influenced by thalamic inhibitory neurons, corticothalamic feedback neurons, and afferent innervation by various brain stem nuclei. Inhibitory innervation of thalamic relay neurons primarily arises from local circuit interneurons and thalamic reticular nucleus (TRN) neurons. Functionally, inhibitory mechanisms contribute to accurate discrimination of visual signals by enhancing surround inhibition of receptive fields (Lee et al. 1994; Livingstone and Hubel 1981) and to the spatial and temporal integration of ascending sensory signals (Berardi and Morrone 1984; Cox and Sherman 2000; Norton and Godwin 1992; Zhu and Uhlrich 1997). In addition to altering sensory information processing, inhibitory mechanisms play an important role in various intrathalamic rhythmic activities associated with different arousal states and pathophysiological conditions such as absence epilepsy (Cox et al. 1997a; Kim et al. 1997; McCormick 2002; Steriade et al. 1993; von Krosigk et al. 1993).

Address for reprint requests and other correspondence: C. L. Cox, Department of Molecular and Integrative Physiology, University of Illinois, 2357 Beckman Institute, 405 North Mathews, Urbana, IL 61801 (cox2@uiuc.edu).

Nitric oxide (NO) has the unconventional characteristic of being a gaseous neurotransmitter (Boehning and Snyder 2003; Garthwaite et al. 1988). Unlike classical neurotransmitters, which are generally spatially restricted near the synapse, NO can behave hormonelike because it can freely move through membranes and influence neighboring neurons several hundred microns away (Garthwaite and Boulton 1995; Park et al. 1998). NO was previously found to produce a variety of actions in the nervous system by altering neuronal excitability and synaptic transmission through modulation of cGMP and S-nitrosylation (Ahern et al. 2002).

Although NO was found to produce a wide variety of actions in many brain regions, NO-mediated actions in the thalamus are predominantly excitatory (Cudeiro and Rivadulla 1999; Salt and Pape 1999). Nitric oxide synthase (NOS), the enzyme required for NO production, is localized within GABAergic dLGN interneurons and TRN neurons and within acetylcholine-containing neurons in mesopontine tegmental nuclei neurons that innervate most thalamic nuclei (Carden et al. 2000; Erisir et al. 1997; Gabbott and Bacon 1994; McCauley et al. 2002, 2003). The NO-releasing compound SIN-1 selectively depolarizes thalamocortical relay neurons by shifting the activation curve of the hyperpolarization-activated mixed cation current I_h (Pape and Mager 1992). Previously NO was shown to selectively potentiate *N*-methyl-D-aspartate (NMDA)–dependent excitatory synaptic responses arising from corticogeniculate afferents in vitro (Alexander et al. 2006). In vivo, the NO precursor L-arginine, the NO donor SIN-1, and cyclic-GMP analogue 8-Br-cGMP potentiate sensory-evoked responses (Do et al. 1994; Shaw and Salt 1997; Shaw et al. 1999). Within the visual system the NO donor SNAP selectively potentiates visual responses mediated by NMDA glutamatergic receptors (Cudeiro and Rivadulla 1999; Cudeiro et al. 1994). Furthermore, extracellular NO concentrations in thalamus are positively correlated with arousal levels, suggesting a putative role in regulating the excitability state of thalamic neurons (Marino and Cudeiro 2003; Williams et al. 1997). Despite the existing work indicating alteration in neuronal excitation and excitatory synaptic transmission, the role of NO in the regulation/modulation of inhibitory activity remains unexplored.

NOS is highly localized in γ-aminobutyric acid (GABA)–containing thalamic neurons as well as afferent cholinergic fibers. In addition, the increase in NO was previously associated with increased GABA release by presynaptic mechanisms in the paraventricular and supraoptic nucleus (Kraus and Prast 2002; Li et al. 2002, 2004; Ohkuma et al. 1998; Ozaki et al. 2000; Yu and Eldred 2005). Considering the thalamic NOS localization and NO-mediated influences on inhibitory activity elsewhere, we sought to test the putative role of NO on inhibitory activity within the thalamus. In addition to reports regarding excitatory actions of NO in thalamus, alterations in inhibitory activity could have a significant influence on accurate visual information transfer. Our results indicate that increasing NO levels potentiated inhibitory activity, presumably increasing GABA release from presynaptic terminals by a cGMP-dependent process. Such an action was further potentiated by the depolarization of TRN, thereby increasing the inhibitory tone in thalamocortical neurons.

METHODS

Brain slice preparation

Sprague–Dawley rats (postnatal age: 10–16 days) were deeply anesthetized with sodium pentobarbital (55 mg/kg); the brains were quickly removed and placed into chilled (4°C), oxygenated (5% CO_2-95% O_2) slicing medium containing (in mM): 2.5 KCl, 1.25 NaH_2PO_4, 10.0 $MgSO_4$, 0.5 $CaCl_2$, 26.0 $NaHCO_3$, 11.0 glucose, and 234.0 sucrose. Slices (300 μm thick) were cut using a vibrating tissue slicer in the coronal plane for dLGN recordings and in the horizontal plane for ventrobasal nucleus (VB) and TRN recordings. Slices were then transferred to a holding chamber containing oxygenated physiological

saline that contained (in mM): 126.0 NaCl, 2.5 KCl, 1.25 NaH_2PO_4, 2.0 $MgCl_2$, 2.0 $CaCl_2$, 26.0 $NaHCO_3$, and 10.0 glucose. Individual slices were then transferred to a recording chamber maintained at 32°C and oxygenated physiological saline was continuously superfused at a rate of 2.0 ml/min.

Intracellular recording procedures

Intracellular recordings were obtained using the whole cell configuration. Recording pipettes had tip resistances of 3–7 MΩ when filled with a solution containing (in mM): 117.0 Cs-gluconate, 13.0 CsCl, 1.0 $MgCl_2$, 0.07 $CaCl_2$, 0.1 EGTA, 10.0 HEPES, 2.0 Na_2-ATP, 0.4 Na-GTP, and 0.3% biocytin. The pH and osmolarity of the intracellular solution was adjusted to 7.3 and 290 mOsm, respectively. The internal solution resulted in a junction potential of approximately 10 mV that was corrected in the voltage measures. A fixed-stage microscope (Axiskop2, Carl Zeiss) equipped with differential interference contrast optics and a ×63 water-immersion objective was used to view individual neurons within the slice. Inhibitory synaptic currents were recorded using an Axoclamp 2B amplifier (Molecular Devices, Sunnyvale, CA) in the continuous voltage-clamp mode and a holding potential of 0 mV. Only neurons with stable access resistances <15 MΩ were included in this study. In current-clamp recordings, K^+ was substituted for Cs^+ in the pipette solution. Membrane voltage was recorded using an Axoclamp 2B amplifier in bridge mode and the active bridge circuit was continuously adjusted to balance the drop in potential produced by passing current through the recording electrode.

Pharmacological agents

Concentrated stock solutions of various pharmacological agents were initially prepared and then diluted in physiological saline to a final concentration before use. Concentrated stocks of 1*H*-[1,2,4]oxadiazolo[4,3-a]quinoxalin-1-one (ODQ) and 3-isobutyl-1-methylxanthine (IBMX) were initially prepared in DMSO. The final DMSO concentration never exceeded 0.1% and this DMSO concentration alone did not produce any alterations in synaptic activity. *N*-(Acetyloxy)-3-nitrosothiovaline (SNAP) was freshly prepared each day at a final concentration in physiological solution. Agonists were applied by a short-duration (1- to 2-min) bolus into the input line of the recording chamber using a syringe pump. All antagonists were bath applied. L-Arginine, SNAP, N^G-monomethyl-L-arginine acetate (L-NMMA), 2-(3-carboxypropyl)-3-amino-6-methoxyphenyl-pyridazinium bromide (SR95531), 2-(4-carboxyphenyl)-4,4,5,5-tetramethylinmidazoline-1-oxide (PTIO), ODQ, TTX, and 8-bromoguanosine cyclic 3′,5′-monophosphate sodium salt (8-Br-cGMP) were purchased from Tocris (Ellisville, MO). IBMX, 8-(4-chlorophenylthio)-guanosine 3′,5′-cyclic monophosphorothioate, and Rp isomer triethylammonium (Rp-CPT-cGMP) were purchased from Sigma (St. Louis, MO).

Data acquisition and analyses

Spontaneous synaptic events were digitized and stored using pCLAMP software (Molecular Devices, Sunnyvale, CA) and analyzed off-line using Mini Analysis software (Synaptosoft, Leonia, NJ). The detection of ISPCs was accomplished by setting a threshold above the baseline level in the presence of the $GABA_A$ antagonist SR95531. Cumulative probability plots were calculated from 30-s windows just before drug application (control) and during the peak drug response, which typically reached a maximum effect approximately 2 min after drug application and leveled off for ≥3 min. The interval across experimental conditions (e.g., in the presence of an antagonist) was constant across experiments. A Kolmogorov–Smirnov (KS) test was used to test statistical significance between different experimental conditions. Histograms illustrating sIPSC frequency and amplitude for individual experiments (e.g., Fig. 1*A*) were constructed using 5-s bins. Time plots illustrating the population data regarding sIPSC frequency and amplitude were constructed

using 30-s bins and then normalized to the predrug baseline level that was calculated from the 3 min before drug application (e.g., Fig. 1*C*). For population data presented as bar graphs, IPSC frequency and amplitude measurements were calculated from 2-min periods before drug application and during the peak drug response. The values for "wash" were calculated from 2-min periods just before the addition of an antagonist or TTX (e.g., see Fig. 1*A*). Data are presented as means ± SE. Most statistical analyses consisted of a Student's *t*-test unless noted otherwise.

RESULTS

In this study, we recorded from 110 thalamocortical neurons, 15 TRN neurons, and four dLGN interneurons. Spontaneous inhibitory postsynaptic currents (sIPSCs) were recorded from dLGN thalamocortical relay neurons. In control conditions, sIPSCs had an overall average amplitude of 24.1 ± 0.1 pA and frequency of 6.5 ± 1.0 Hz (n = 30 neurons). The NO donor SNAP (500 μM) produced a long-lasting, robust increase in sIPSC activity that usually returned to baseline levels within 20 min (Fig. 1, *A* and *B*). The sIPSCs were completely blocked by bath application of the $GABA_A$ antagonist SR95531 (10 μM), indicating these synaptic events were mediated by $GABA_A$ receptors (Fig. 1, *A* and *B*, +SR95531). SNAP (20–500 μM) produced a concentration-dependent increase in sIPSC frequency (Fig. 1, *C* and *D*, $P < 0.01$, ANOVA with Tukey–Kramer multiple comparisons). At the lowest concentration tested, SNAP (20 μM) did not significantly alter sIPSC frequency or amplitude above baseline conditions (Fig. 1*D*, $n = 7$, $P > 0.1$, paired *t*-test). At higher concentrations, SNAP (100, 500 μM) produced a significant increase in sIPSC frequency above baseline levels (Fig. 1, *C* and *D*). SNAP (100 μM) increased the peak sIPSC frequency to 139.4 ± 11.4% of control (predrug: 5.2 ± 0.7 Hz, SNAP: 7.0 ± 0.9 Hz, $n = 7$, $P < 0.01$, paired *t*-test). SNAP (500 μM) increased sIPSC frequency to 140.4 ± 10.1% of control (predrug: 6.5 ± 0.8 Hz, SNAP: 8.8 ± 1.1 Hz, $n = 17$, $P < 0.01$, paired *t*-test). The higher concentrations of SNAP tested (100, 500 μM) did not significantly differ from each other, but did significantly differ from 20 μM SNAP ($P < 0.01$, Tukey–Kramer multiple comparisons). In contrast to frequency, sIPSC amplitudes were not significantly altered at any SNAP concentration tested (Fig. 1*D*, $P > 0.1$, paired *t*-test).

GABAergic innervation of dLGN relay neurons arises from TRN neurons and local dLGN interneurons. We next tested whether SNAP altered the excitability of TRN neurons or dLGN interneurons. Current-clamp recordings were obtained from 15 TRN neurons that had an average resting membrane potential of −79.0 ± 3.8 mV and apparent input resistance of 167.8 ± 36.6 MΩ. SNAP (500 μM) produced a long-lasting depolarization that averaged 3.6 ± 1.2 mV in 13 of 15 neurons tested (Fig. 2*A*). The depolarization recovered to baseline levels within 14 min. We next obtained current-clamp recordings from four dLGN interneurons. These neurons were differentiated by their unique intrinsic properties and post hoc from their distinct morphology (Govindaiah and Cox 2004;Pape and McCormick 1995;Williams et al. 1996). Interneurons had a lower resting membrane potential of −64.3 ± 5.0 mV ($P < 0.01$, paired *t*-test) and a greater input resistance averaging 461.5 ± 121.2 MΩ ($P < 0.01$, paired *t*-test) compared with TRN neurons. In the interneurons, SNAP (500 μM) did not alter the membrane potential or input resistance (Fig. 2*B*, $n = 4$), indicating that the SNAP-mediated increase in sIPSC frequency in relay neurons could result from suprathreshold excitation of TRN neurons.

To determine if the increase in sIPSC activity results from suprathreshold excitation of TRN neurons, we tested whether the SNAP-mediated increase in sIPSC frequency in relay neurons was blocked in the presence of tetrodotoxin (TTX). In control conditions, SNAP (500 μM) increased sIPSC frequency with no apparent change in amplitude (Fig. 3, *A* and *B*). As illustrated in Fig. 3*C*, SNAP produced a significant decrease in interevent intervals (*P*

< 0.01, KS test) with no change in sIPSC amplitude ($P > 0.1$, KS test). After the addition of TTX (0.5 μM), SNAP (500 μM) still produced a significant increase in sIPSC frequency (Fig. 3, *A*, *B*, and *C*, $P < 0.01$, KS test). In the overall population, in control conditions SNAP produced an increase in sIPSC frequency that averaged 145.2 ± 9.9% of baseline levels (Fig. 3, *D* and *E*, $n = 10$, $P < 0.01$, paired *t*-test) with no change in sIPSC amplitude. In the presence of TTX, SNAP produced an increase in IPSC frequency that averaged 140.5 ± 16.0% of baseline levels (Fig. 3, *D* and *E*, $n = 10$). The peak increase in IPSC frequency produced by SNAP in TTX did not differ significantly from that in control conditions (Fig. 3*E*, $P > 0.1$, *t*-test). These results indicate that the SNAP-mediated potentiation does not result from the suprathreshold excitation of TRN neurons or interneurons. The increase in sIPSC activity is consistent with a presynaptic action, likely arising from axonal terminals of either TRN neurons or interneurons, or from presynaptic dendrites of interneurons (Cox et al. 1998; Govindaiah and Cox 2004).

To evaluate the effects of endogenously synthesized NO on inhibitory activity, we next used the nitric oxide synthase (NOS) substrate L-arginine. In TTX (0.5 μM), L-arginine (1 mM, 2 min) produced an increase in IPSC frequency in 16 of 24 relay cells tested (Fig. 4, *A* and *B*). Overall, L-arginine produced a peak increase in sIPSC frequency that averaged 120.6 ± 3.3% of baseline levels (Fig. 4*C*, $n = 24$, $P < 0.01$, paired *t*-test). As with the SNAP-mediated actions, there was no alteration in IPSC amplitude (Fig. 4*C*). The inactive form of arginine, D-arginine, did not alter IPSC frequency (92.9 ± 7.0% of baseline level, $n = 5$, $P > 0.1$, paired *t*-test).

We next tested whether the specific NO scavenger PTIO could antagonize the SNAP-mediated potentiation of IPSC activity in relay neurons. First, we tested whether the SNAP-mediated increase in sIPSC activity was repeatable. The potentiation in sIPSC frequency produced by the first SNAP application (146.2 ± 11.8% of baseline level, $n = 4$) did not differ from the second SNAP application at a 20-min interval (149.5 ± 9.2%, $P > 0.1$, paired *t*-test). In a different subpopulation of relay neurons, the initial SNAP (500 μM) application produced a peak increase in IPSC frequency that averaged 152.5 ± 16.0% of control ($n = 7$). In PTIO (20 μM), the SNAP-mediated increase in mIPSC frequency was significantly decreased and did not differ from baseline levels (Fig. 5*A*, $n = 7$, $P > 0.1$, paired *t*-test). In addition, PTIO (20 μM) alone did not alter sIPSC activity (Fig. 5*Aiii*, $P > 0.1$, paired *t*-test).

Because L-arginine requires NOS to produce NO, we next tested the NOS inhibitor L-NMMA on the L-arginine–mediated actions. In control conditions (TTX, 0.5 μM), the initial application of L-arginine produced an increase in sIPSC frequency that averaged 146.6 ± 7.3% ($n = 6$) of baseline levels (Fig. 5*B*). In L-NMMA (100 μM), the subsequent application of L-arginine increased the sIPSC frequency (116.9 ± 10.1%), significantly less than the response to the initial L-arginine application ($P < 0.01$, paired *t*-test). L-NMMA alone did not alter sIPSC frequency (Fig. 5*Biii*). Furthermore, there were no alterations in sIPSC amplitude by L-arginine or L-NMMA.

NO was previously reported to engage multiple intracellular messenger systems including the guanylyl cyclase (GC)/cGMP pathway (Boehning and Snyder 2003; Bredt and Snyder 1989). We next tested whether the guanylyl cyclase inhibitor ODQ could attenuate the SNAP-mediated facilitation of inhibitory activity. In TTX (0.5 μM), SNAP (500 μM) produced a significant increase in sIPSC frequency that averaged 140.9 ± 10.8% of baseline levels (Fig. 6*A*, $P < 0.01$, paired *t*-test, $n = 7$). The subsequent SNAP application in ODQ failed to alter sIPSC frequency (Fig. 6*A*, 98.6 ± 7.5%, $P > 0.1$, paired *t*-test, $n = 7$). The addition of ODQ (100 μM) alone did not alter sIPSC activity (Fig. 6*Aii*, $P > 0.1$, paired *t*-test). These results suggest that NO exerts its effect through activation of soluble guanylyl cyclase (sGC) to increase the cGMP levels in thalamus.

To test whether a general increase in cGMP level mimics the SNAP-mediated action, we bath-applied the membrane permeable cyclic-GMP analogue, 8-bromo-cyclic-GMP (8Br-cGMP). In TTX (0.5 μM), 8Br-cGMP (50 μM, 2 min) did not significantly alter sIPSC frequency (Fig. 6*Bi*, 105.9 ± 13.0%, $P > 0.1$, paired *t*-test, $n = 5$). However, in the presence of a phosphodiesterase inhibitor, IBMX (100 μM), which inhibits cyclic nucleotide degradation (Li et al. 2002;Yawo 1999), 8Br-cGMP (50 μM) produced a significant potentiation in sIPSC frequency (Fig. 6*B*, *ii* and *iv*, 139.0 ± 11.4%, $P < 0.01$, paired *t*-test, $n = 8$), which did not reverse within 30 min after drug application. IBMX (100 μM) alone, before 8Br-cGMP application, did not significantly alter sIPSC frequency (98.0 ± 6.5%, $n = 21$, $P > 0.1$, paired *t*-test). Increasing the 8Br-cGMP concentration to 1 mM in the presence of IBMX produced a shorter-latency facilitation with a maximum effect similar to that of the lower 8Br-cGMP concentration (Fig. 6*B*, *iii* and *iv*, 135.0 ± 12.3%, $n = 13$, $P < 0.01$, paired *t*-test).

One of the targets for cGMP activity is the cGMP-stimulated protein kinase G (PKG) (Jaffrey and Snyder 1995) and this pathway is involved with increased GABA release in the paraventricular nucleus (Li et al. 2004). Furthermore, type II cyclic-GMP–dependent protein kinase was previously reported to be highly distributed in thalamus, so we next tested whether the membrane-permeable PKG inhibitor Rp-pCPT-cGMP could attenuate the 8Br-Cgmp–mediated increase in sIPSC frequency (Bladen et al. 1996; El Husseini et al. 1999). In the presence of Rp-pCPT-cGMP (5 μM) and IBMX (100 μM), 8Br-cGMP (1 mM) still produced a significant increase in sIPSC frequency (126.9 ± 7.5%, $n = 4$, $P < 0.01$, paired *t*-test) and this increase did not differ from the 8Br-cGMP–mediated facilitation in control conditions ($P > 0.05$).

Our data strongly indicate that activation of the NO system enhances inhibitory activity by a presynaptic mechanism. Inhibitory innervation of dLGN relay neurons arises from three sources. The local circuit interneurons innervated relay neurons by presynaptic dendrites (named F2 terminals) and axon terminals (named F1 terminals) (Famiglietti Jr and Peters 1972; Guillery 1969; Hamos et al. 1985; Montero 1986; Ralston 1971). TRN neurons also innervate relay neurons by axonal terminals (F1 terminals). To distinguish these two sources of innervation (interneuron vs. TRN neuron), we next recorded from ventrobasal nucleus (VB), a structure that contains very few GABAergic local circuit interneurons in rodents and therefore lacks F2 terminals (Arcelli et al. 1997; Ottersen and Storm-Mathisen 1984). In this preparation, sIPSCs arise from axon terminals of TRN neurons (F1 terminals). As illustrated in Fig. 7*A*, in control conditions SNAP (500 μM) increased the sIPSC frequency with little apparent change in sIPSC amplitude (Fig. 7,*A* and *B*). After the addition of TTX (0.5 μM), the facilitation by SNAP persisted, but to a lesser extent than in control conditions (Fig. 7, *A* and *B*). This TTX-sensitive component within VB likely arises from suprathreshold excitation of TRN neurons (e.g., see Fig. 2*A*) that remain synaptically intact in the horizontal thalamic slice. As indicated in the cumulative probability plots, there was a significant decrease in the interevent intervals in the presence of SNAP in control and TTX conditions (Fig. 7*C*, $P < 0.01$, KS test). Similarly, the population data indicate that SNAP significantly increased the sIPSC frequency an average of 133.5 ± 7.5% of control (Fig. 6, *D* and *E*, $P < 0.01$, paired *t*-test) and in TTX, SNAP produced a peak increase in sIPSC activity that averaged 118.6 ± 4.8%, which was significantly greater than baseline levels (Fig. 6, *D* and *E*, $P < 0.05$, paired *t*-test, $n = 9$). Notable was a statistical difference of the SNAP-mediated frequency potentiation in TTX between LGN and VB relay cells (140.5 ± 16.0 vs. 118.6 ± 4.8%, $P < 0.01$). Unlike dLGN neurons, SNAP produced a significant increase in sIPSC amplitude in the control conditions (Fig. 6*C*, $P < 0.01$, KS test). The population data support the increase of sIPSC amplitude that averaged 109.0 ± 2.1% (Fig. 6, *D* and *E*, $P < 0.01$, paired *t*-test, $n = 9$), suggesting that a portion of increased sIPSCs resulted from suprathreshold depolarization of TRN neurons by SNAP.

DISCUSSION

In this study, we investigated the influence of NO on inhibitory synaptic activity within the thalamus based on previous anatomical studies indicating NOS localization in GABAergic thalamic neurons (Erisir et al. 1997; McCauley et al. 2002, 2003). To summarize, we found that the NO donor SNAP or the NO precursor L-arginine significantly increased spontaneous GABA-mediated inhibitory activity in thalamic relay neurons by enhancing the frequency—but not the amplitude—of the IPSCs. The specific NO scavenger carboxyl-PTIO attenuated SNAP-mediated potentiation and the NOS inhibitor, L-NMMA acetate, decreased the L-arginine–mediated potentiation. These NO-mediated actions appear to be involved in an increase of the cGMP level because the soluble guanylyl cyclase inhibitor ODQ attenuated the SNAP-mediated potentiation. Furthermore, the increase in IPSC frequency was mimicked by the cGMP analogue 8-Br-cGMP, in the presence of the phosphodiesterase inhibitor IBMX. The augmentation of inhibitory activity by SNAP was present in both dLGN and VB relay neurons, but was significantly less in VB neurons. The VB nucleus, unlike the dLGN, lacks local circuit interneurons and receives most of its inhibitory innervation from TRN neurons. Thus our data indicate that NO leads to an increase in GABA release from presynaptic terminals of TRN neurons and likely local circuit neurons as well, thereby increasing the inhibitory drive onto thalamic relay neurons.

cGMP dependency of presynaptic NO actions

Based on our results, the NO-mediated increase in inhibitory activity results from an increase in GABA release by presynaptic mechanisms. In our experiments, the sIPSC frequency was significantly increased by NO agonists; however, the sIPSC amplitude was unaltered. Furthermore, the increase in sIPSC frequency persisted in TTX, indicating suprathreshold excitation of presynaptic GABA-containing neurons (i.e., TRN neurons) was not required. Such a presynaptic mechanism is consistent with the NO actions reported in other brain regions including paraventricular nucleus of the hypothalamus, supraoptic neurons, nucleus accumbens, cultured neocortical neurons, and retinal neurons (Kraus and Prast 2002; Li et al. 2002; Ohkuma et al. 1998; Ozaki et al. 2000; Yu and Eldred 2005). Most NO-mediated actions described thus far in the CNS involve either cGMP or S-nitrosylation (Ahern et al. 2002) and our results appear dependent on the cGMP pathway. The cGMP analogue 8-Br-cGMP, in presence of the phosphodiesterase inhibitor IBMX, increased sIPSC frequency and the SNAP-mediated increase in sIPSC activity was inhibited by the guanylyl cyclase inhibitor ODQ.

The increase in cGMP produced by NO can target cGMP-gated channels (Ingram and Williams 1996; Zagotta and Siegelbaum 1996), cGMP-dependent phosphodiesterases (Kraus and Prast 2002), and cGMP-dependent PKG (Jaffrey and Snyder 1995). Despite the presence of type II cyclic GMP-dependent PKG within thalamic neurons, the selective inhibitor Rp-pCPT-cGMP did not attenuate the SNAP-mediated actions (Bladen et al. 1996). Furthermore, the increase in inhibitory activity also persisted in the presence of the phosphodiesterase inhibitor IBMX. Assuming the lack of PKG and phosphodiesterase involvement, one possible mechanism is that cGMP directly activates cGMP-gated channels in the presynaptic terminal, leading to transmitter release. One candidate is the hyperpolarization-activated mixed-cation current I_h; the HCN channels that mediate I_h have binding sites for cGMP and cAMP (Zagotta et al. 2003). Moreover, I_h contributes to increased GABA release in presynaptic terminals of cerebellar basket cells (Southan et al. 2000). Therefore the increase in cGMP produced by NO could potentiate HCN channels in the axon terminals or dendrite of inhibitory neurons (TRN and dLGN interneuron), leading to the increase of GABA release. However, at this point, we cannot definitively exclude the role of PKG because our highest Rp-pCPT-cGMP concentration tested (5 μM) may not completely block all PKG-mediated activities, although a lower concentration (1 μM) was

used to completely block SNAP-mediated inhibitory actions in a slice preparation of rat paraventricular nucleus (Li et al. 2004). Furthermore, the cGMP pathway also appears to be involved in the postsynaptic depolarization of dLGN thalamic relay neurons by NO and the facilitation of excitatory synaptic responses arising from corticogeniculate afferents (Alexander et al. 2006; Pape and Mager 1992; Shaw et al. 1999). However, it is important to note the negligible effects of 8-Br-cGMP reported from in vivo single-unit recordings in cat dLGN, suggesting potential diversity in NO-mediated actions in the thalamus (Cudeiro et al. 1994).

Sources and target sites of NO in the thalamus

One potential source of NO in the thalamus arises from acetylcholine-containing brain stem nuclei. Cholinergic neurons arising from the parabrachial region of the brain stem that innervate dLGN also contain NOS (Carden et al. 2000; Erisir et al. 1997). Activity of the parabrachial neurons is positively correlated with arousal levels and therefore increased levels of NO-mediated actions may be correlated with increasing arousal levels (Williams et al. 1997). In addition, these cholinergic neurons also innervate presynaptic GABA-containing dendrites of dLGN interneurons that form dendrodendritic synapses onto relay cell dendrites, often forming a characteristic “triadic” junction (F2 terminal) (Famiglietti Jr and Peters 1972; Guillery 1969; Hamos et al. 1985; Montero 1986; Ralston 1971). Thus NO may provide an effective output control of presynaptic dendrites of local interneurons (Cox and Sherman 2000; Govindaiah and Cox 2004). Another possible source of NO is from GABA-containing neurons in the thalamus. NOS and GABA are co-localized in a subpopulation of local inhibitory interneurons in the cat dLGN (Erisir et al. 1997; McCauley et al. 2003).

Considering the innervation of TRN by cholinergic neurons of the parabrachial region, the TRN is another site for NO-mediated actions. In addition, recent evidence indicates that NOS is also expressed in TRN of ferrets (McCauley et al. 2002). Our data indicate that increased NO activity leads to depolarization of TRN neurons (Fig. 2) and increased GABA release from presynaptic terminals of TRN neurons (Fig. 7). These experiments are the first electrophysiological observations suggesting that TRN neurons may be a target for endogenous NO. The activation of TRN neurons plays an important role in oscillations of thalamocortical systems shown during the sleep cycle (Cox et al. 1997b; McCormick 2002; Steriade et al. 1993; von Krosigk et al. 1993). Furthermore, NO is also an easy diffusible substance that can reach several hundred microns (Garthwaite and Boulton 1995; Park et al. 1998), presumably acting as a spatial signal simultaneously influencing a large neuronal population by local diffusion in thalamus. Therefore the widespread effects for functional control of neural networks without direct synaptic connections could be indicative of NO action in thalamus. These properties may endow the NO system with important functions in controlling sensory transfer and thalamic oscillatory activity in a global manner.

Functional role of NO in the visual thalamus

Considering GABA-mediated inhibition can have important influences on visual information processing in the thalamus, alterations in inhibitory activity by NO could significantly influence such processing. GABA-mediated inhibition was previously reported to be involved in accurate discrimination of incoming signals and enhancing sensitivity for local contrast information (Berardi and Morrone 1984; Govindaiah and Cox 2004; Holdefer et al. 1989; Livingstone and Hubel 1981; Norton and Godwin 1992; Sillito and Kemp 1983). GABA-mediated activity appears to regulate receptive field sensitivity (Holdefer et al. 1989; Norton et al. 1989). Lesions of TRN neurons increase receptive field size in somatosensory thalamic neurons, suggesting a surround antagonistic role of TRN neurons (Lee et al. 1994). The increment of contrast caused the increasing response of LGN target cells using

extracellular single-unit recording (Kaplan et al. 1987). From this, we would predict that the inhibitory action of NO could play an important role on contrast information by regulating receptive field size and/or sensitivity.

Previous in vivo studies indicate that NO leads to an enhancement of sensory-evoked responses in presumed thalamic relay neurons (Cudeiro et al. 1994; Shaw et al. 1999). Although there is some controversy regarding the role of cGMP underlying the facilitation, (Shaw et al. 1999) found a striking similarity between the actions of NO agonists and cGMP, whereas Cudeiro et al. (1994) found negligible actions of cGMP activation. In vitro studies found postsynaptic depolarizations produced by NO agents in thalamic relay neurons, consistent with the excitatory effects of NO (Pape and Mager 1992). Our data provide a novel role of NO within the thalamus—that is, activation of NO by a cGMP-dependent pathways leads to a presynaptic enhancement of inhibitory activity that occurs independent of the action potential discharge of GABA-containing neurons. Depending on the spatial distribution of NO, such changes may provide a mechanism to sharpen the excitatory relay through the thalamus. Our working hypothesis is that with attentive states, increased output of NOS-containing cholinergic neurons would lead to increased NO synthesis and release, thereby leading to a direct postsynaptic depolarization decreasing the threshold for suprathreshold excitation through the thalamic relay and, at the same time, NO would lead to increased inhibitory activity that would in turn enhance surround antagonistic actions, ultimately increasing the signal-to-noise ratio and potentially sharpening receptive fields. Therefore we would speculate that NO may be crucial for sharpening visual transmission through potentiation of GABA release accompanied with the facilitation of sensory transmission.

Acknowledgments

We thank B. Wilson and Drs. S. Lee, G. Govindaiah, and K. Paul for valuable comments on this manuscript.

GRANTS

This research was supported by the National Eye Institute Grant EY-014024.

REFERENCES

Ahern GP, Klyachko VA, Jackson MB. cGMP and S-nitrosylation: two routes for modulation of neuronal excitability by NO. Trends Neurosci 2002;25:510–517. [PubMed: 12220879]

Alexander GM, Kurukulasuriya NC, Mu J, Godwin DW. Cortical feedback to the thalamus is selectively enhanced by nitric oxide. Neuroscience 2006;142:223–234. [PubMed: 16876956]

Arcelli P, Frassoni C, Regondi MC, De Biasi S, Spreafico R. GABAergic neurons in mammalian thalamus: a marker of thalamic complexity? Brain Res Bull 1997;42:27–37. [PubMed: 8978932]

Berardi N, Morrone MC. The role of gamma-aminobutyric acid mediated inhibition in the response properties of cat lateral geniculate nucleus neurones. J Physiol 1984;357:505–523. [PubMed: 6512702]

Bladen C, Loewen D, Vincent SR. Autoradiographic localization of [3H]-cyclic GMP binding sites in the rat brain. J Chem Neuroanat 1996;10:287–293. [PubMed: 8811419]

Boehning D, Snyder SH. Novel neural modulators. Annu Rev Neurosci 2003;26:105–131. [PubMed: 14527267]

Bredt DS, Snyder SH. Nitric oxide mediates glutamate-linked enhancement of cGMP levels in the cerebellum. Proc Natl Acad Sci USA 1989;86:9030–9033. [PubMed: 2573074]

Carden WB, Datskovskaia A, Guido W, Godwin DW, Bickford ME. Development of the cholinergic, nitrergic, and GABAergic innervation of the cat dorsal lateral geniculate nucleus. J Comp Neurol 2000;418:65–80. [PubMed: 10701756]

Cox CL, Huguenard JR, Prince DA. Nucleus reticularis neurons mediate diverse inhibitory effects in thalamus. Proc Natl Acad Sci USA 1997a;94:8854–8859. [PubMed: 9238067]

Cox CL, Huguenard JR, Prince DA. Peptidergic modulation of intrathalamic circuit activity *in vitro*: actions of cholecystokinin. J Neurosci 1997b;17:70–82. [PubMed: 8987737]

Cox CL, Sherman SM. Control of dendritic outputs of inhibitory interneurons in the lateral geniculate nucleus. Neuron 2000;27:597–610. [PubMed: 11055441]

Cox CL, Zhou Q, Sherman SM. Glutamate locally activates dendritic outputs of thalamic interneurons. Nature 1998;394:478–482. [PubMed: 9697770]

Cudeiro J, Grieve KL, Rivadulla C, Rodrgíuez R, Martínez-Conde S, Acuña C. The role of nitric oxide in the transformation of visual information within the dorsal lateral geniculate nucleus of the cat. Neuropharmacology 1994;33:1413–1418. [PubMed: 7532823]

Cudeiro J, Rivadulla C. Sight and insight—on the physiological role of nitric oxide in the visual system. Trends Neurosci 1999;22:109–116. [PubMed: 10199635]

Do K-Q, Binns KE, Salt TE. Release of the nitric oxide precursor, arginine, from the thalamus upon sensory afferent stimulation, and its effect on thalamic neurons *in vivo*. Neuroscience 1994;60:581–586. [PubMed: 7523982]

El Husseini AE, Williams J, Reiner PB, Pelech S, Vincent SR. Localization of the cGMP-dependent protein kinases in relation to nitric oxide synthase in the brain. J Chem Neuroanat 1999;17:45–55. [PubMed: 10569239]

Erisir A, Van Horn SC, Bickford ME, Sherman SM. Immunocytochemistry and distribution of parabrachial terminals in the lateral geniculate nucleus of the cat: a comparison with corticogeniculate terminals. J Comp Neurol 1997;377:535–549. [PubMed: 9007191]

Famiglietti EV Jr, Peters A. The synaptic glomerulus and the intrinsic neuron in the dorsal lateral geniculate nucleus of the cat. J Comp Neurol 1972;144:285–334. [PubMed: 4112778]

Gabbott PLA, Bacon SJ. Two types of interneuron in the dorsal lateral geniculate nucleus of the rat: a combined NADPH diaphorase histochemical and GABA immunocytochemical study. J Comp Neurol 1994;350:281–301. [PubMed: 7884043]

Garthwaite J, Boulton CL. Nitric oxide signaling in the central nervous system. Annu Rev Physiol 1995;57:683–706. [PubMed: 7539993]

Garthwaite J, Charles SL, Chess-Williams R. Endothelium-derived relaxing factor release on activation of NMDA receptors suggests role as intercellular messenger in the brain. Nature 1988;336:385–388. [PubMed: 2904125]

Govindaiah, Cox CL. Synaptic activation of metabotropic glutamate receptors regulates dendritic outputs of thalamic interneurons. Neuron 2004;41:611–623. [PubMed: 14980209]

Guillery RW. The organization of synaptic interconnections in the laminae of the dorsal lateral geniculate nucleus of the cat. Z Zellforsch Mikroskop Anat 1969;96:1–38.

Hamos JE, Van Horn SC, Raczkowski D, Uhlrich DJ, Sherman SM. Synaptic connectivity of a local circuit neurone in lateral geniculate nucleus of the cat. Nature 1985;317:618–621. [PubMed: 4058571]

Holdefer RN, Norton TT, Godwin DW. Effects of bicuculline on signal detectability in lateral geniculate nucleus relay cells. Brain Res 1989;488:341–347. [PubMed: 2743129]

Ingram SL, Williams JT. Modulation of the hyperpolarization-activated current (Ih) by cyclic nucleotides in guinea-pig primary afferent neurons. J Physiol 1996;492:97–106. [PubMed: 8730586]

Jaffrey SR, Snyder SH. Nitric oxide: a neural messenger. Annu Rev Cell Dev Biol 1995;11:417–440. [PubMed: 8689564]

Kaplan E, Purpura K, Shapley RM. Contrast affects the transmission of visual information through the mammalian lateral geniculate nucleus. J Physiol 1987;391:267–288. [PubMed: 2832591]

Kim U, Sanchez-Vives MV, McCormick DA. Functional dynamics of GABAergic inhibition in the thalamus. Science 1997;278:130–134. [PubMed: 9311919]

Kraus MM, Prast H. Involvement of nitric oxide, cyclic GMP and phosphodiesterase 5 in excitatory amino acid and GABA release in the nucleus accumbens evoked by activation of the hippocampal fimbria. Neuroscience 2002;112:331–343. [PubMed: 12044451]

Lee SM, Friedberg MH, Ebner FF. The role of GABA-mediated inhibition in the rat ventral posterior medial thalamus. I. Assessment of receptive field changes following thalamic reticular nucleus lesions. J Neurophysiol 1994;71:1702–1715. [PubMed: 8064343]

Li DP, Chen SR, Finnegan TF, Pan HL. Signalling pathway of nitric oxide in synaptic GABA release in the rat paraventricular nucleus. J Physiol 2004;554:100–110. [PubMed: 14678495]

Li DP, Chen SR, Pan HL. Nitric oxide inhibits spinally projecting paraventricular neurons through potentiation of presynaptic GABA release. J Neurophysiol 2002;88:2664–2674. [PubMed: 12424302]

Livingstone MS, Hubel DH. Effects of sleep and arousal on the processing of visual information in the cat. Nature 1981;291:554–561. [PubMed: 6165893]

Marino J, Cudeiro J. Nitric oxide-mediated cortical activation: a diffuse wake-up system. J Neurosci 2003;23:4299–4307. [PubMed: 12764118]

McCauley AK, Carden WB, Godwin DW. Brain nitric oxide synthase expression in the developing ferret lateral geniculate nucleus: analysis of time course, localization, and synaptic contacts. J Comp Neurol 2003;462:342–354. [PubMed: 12794737]

McCauley AK, Meyer GA, Godwin DW. Developmental regulation of brain nitric oxide synthase expression in the ferret thalamic reticular nucleus. Neurosci Lett 2002;320:151–155. [PubMed: 11852184]

McCormick DA. Cortical and subcortical generators of normal and abnormal rhythmicity. Int Rev Neurobiol 2002;49:99–114. [PubMed: 12040908]

Montero VM. Localization of gamma-aminobutyric acid (GABA) in type 3 cells and demonstration of their source to F2 terminals in the cat lateral geniculate nucleus: a Golgi-electron-microscopic GABA-immunocytochemical study. J Comp Neurol 1986;254:228–245. [PubMed: 3540041]

Norton TT, Godwin DW. Inhibitory GABAergic control of visual signals at the lateral geniculate nucleus. Prog Brain Res 1992;90:193–217. [PubMed: 1631300]

Norton TT, Holdefer RN, Godwin DW. Effects of bicuculline on receptive field center sensitivity of relay cells in the lateral geniculate nucleus. Brain Res 1989;488:348–352. [PubMed: 2743130]

Ohkuma S, Katsura M, Hibino Y, Hara A, Shirotani K, Ishikawa E, Kuriyama K. Mechanisms for facilitation of nitric oxide-evoked [3H]GABA release by removal of hydroxyl radical. J Neurochem 1998;71:1501–1510. [PubMed: 9751183]

Ottersen OP, Storm-Mathisen J. GABA-containing neurons in the thalamus and pretectum of the rodent. An immunocytochemical study. Anat Embryol 1984;170:197–207. [PubMed: 6517354]

Ozaki M, Shibuya I, Kabashima N, Isse T, Noguchi J, Ueta Y, Inoue Y, Shigematsu A, Yamashita H. Preferential potentiation by nitric oxide of spontaneous inhibitory postsynaptic currents in rat supraoptic neurones. J Neuroendocrinol 2000;12:273–281. [PubMed: 10718923]

Pape H-C, Mager R. Nitric oxide controls oscillatory activity in thalamocortical neurons. Neuron 1992;9:441–448. [PubMed: 1326294]

Pape H-C, McCormick DA. Electrophysiological and pharmacological properties of interneurons in the cat dorsal lateral geniculate nucleus. Neuroscience 1995;68:1105–1125. [PubMed: 8544986]

Park JH, Straub VA, O'Shea M. Anterograde signaling by nitric oxide: characterization and in vitro reconstitution of an identified nitrergic synapse. J Neurosci 1998;18:5463–5476. [PubMed: 9651227]

Ralston HJ. Evidence for presynaptic dendrites and a proposal for their mechanism of action. Nature 1971;230:585–587. [PubMed: 4101752]

Salt TE, Pape HC. On the role of NO in the thalamus. Trends Neurosci 1999;22:388–389. [PubMed: 10441296]

Shaw PJ, Charles SL, Salt TE. Actions of 8-bromo-cyclic-CMP on neurones in the rat thalamus in vivo and in vitro. Brain Res 1999;833:272–277. [PubMed: 10375703]

Shaw PJ, Salt TE. Modulation of sensory and excitatory amino acid responses by nitric oxide donors and glutathione in the ventrobasal thalamus of the rat. Eur J Neurosci 1997;9:1507–1513. [PubMed: 9240408]

Sillito AM, Kemp JA. The influence of GABAergic inhibitory processes on the receptive field structure of X and Y cells in cat dorsal lateral geniculate nucleus (dLGN). Brain Res 1983;277:63–77. [PubMed: 6640295]

Southan AP, Morris NP, Stephens GJ, Robertson B. Hyperpolarization-activated currents in presynaptic terminals of mouse cerebellar basket cells. J Physiol 2000;526:91–97. [PubMed: 10878102]

Steriade M, McCormick DA, Sejnowski TJ. Thalamocortical oscillations in the sleeping and aroused brain. Science 1993;262:679–685. [PubMed: 8235588]

von Krosigk M, Bal T, McCormick DA. Cellular mechanisms of a synchronized oscillation in the thalamus. Science 1993;261:361–364. [PubMed: 8392750]

Williams JA, Vincent SR, Reiner PB. Nitric oxide production in rat thalamus changes with behavioral state, local depolarization, and brainstem stimulation. J Neurosci 1997;17:420–427. [PubMed: 8987767]

Williams SR, Turner JP, Anderson CM, Crunelli V. Electrophysiological and morphological properties of interneurones in the rat dorsal lateral geniculate nucleus *in vitro*. J Physiol 1996;490:129–147. [PubMed: 8745283]

Yawo H. Involvement of cGMP-dependent protein kinase in adrenergic potentiation of transmitter release from the calyx-type presynaptic terminal. J Neurosci 1999;19:5293–5300. [PubMed: 10377340]

Yu D, Eldred WD. Nitric oxide stimulates gamma-aminobutyric acid release and inhibits glycine release in retina. J Comp Neurol 2005;483:278–291. [PubMed: 15682393]

Zagotta WN, Olivier NB, Black KD, Young EC, Olson R, Gouaux E. Structural basis for modulation and agonist specificity of HCN pacemaker channels. Nature 2003;425:200–205. [PubMed: 12968185]

Zagotta WN, Siegelbaum SA. Structure and function of cyclic nucleotidegated channels. Annu Rev Neurosci 1996;19:235–263. [PubMed: 8833443]

Zhu JJ, Uhlrich DJ. Nicotinic receptor-mediated responses in relay cells and interneurons in the rat lateral geniculate nucleus. Neuroscience 1997;80:191–202. [PubMed: 9252231]

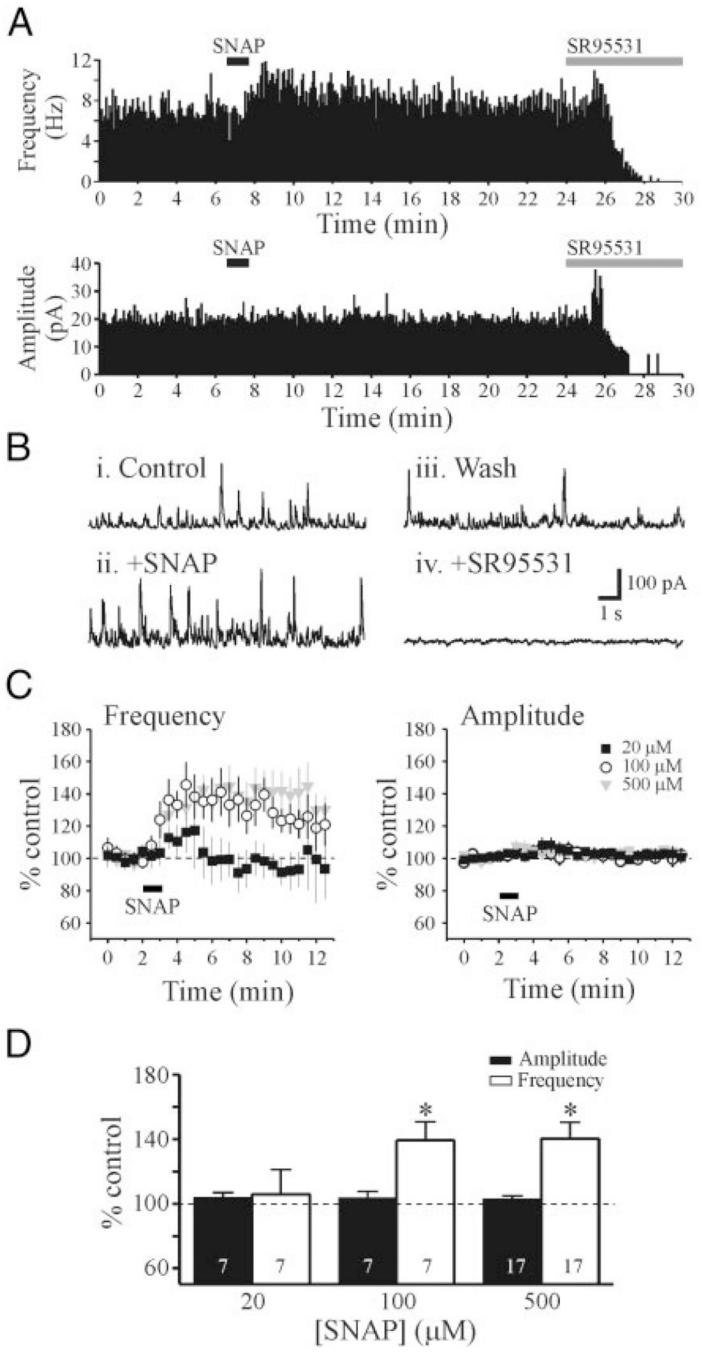

FIG. 1.

SNAP [*N*-(acetyloxy)-3-nitrosothiovaline] potentiates inhibitory activity in a voltage-clamp recording from a dorsal lateral geniculate nucleus (dLGN) relay neuron. *A*: histograms showing the frequency and amplitude of spontaneous inhibitory postsynaptic currents (sIPSCs) in artificial cerebrospinal fluid (ACSF), after SNAP application (500 µM), wash, and in SR95531 [2-(3-carboxypropyl)-3-amino-6-methoxyphenyl-pyridazinium bromide, 10 µM]. Histograms here and in subsequent figures were constructed using 5-s bins. *B*: representative traces in control conditions, after SNAP application, wash, and in the presence of SR95531 from neuron in *A*. Note the increase in frequency of outward (inhibitory) events after SNAP application. After recovery of the SNAP-mediated response,

SR95531 completely attenuated the sIPSCs. *C*: population data for 3 different SNAP concentrations (20 μM, $n = 7$; 100 μM, $n = 7$; and 500 μM, $n = 17$). *D*: these graphs illustrate the peak effect of SNAP on sIPSC amplitude (filled bar) and frequency (open bar). $*P < 0.01$.

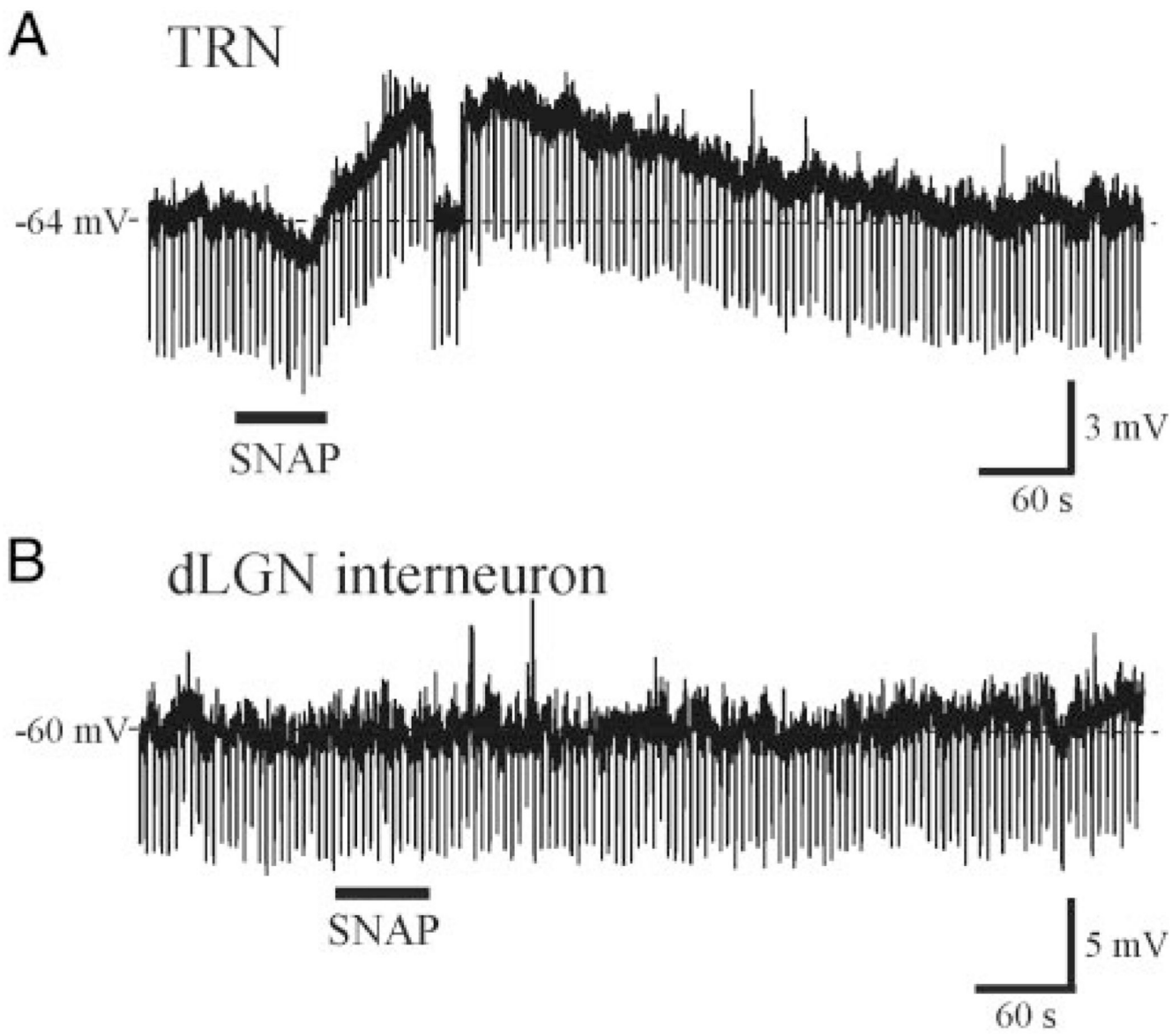

FIG. 2.

SNAP depolarizes thalamic reticular nucleus (TRN) neurons, but not local dLGN interneurons. *A*: current-clamp recording from a TRN neuron. SNAP (500 μM, solid bar) produced a long-lasting membrane depolarization (~4 mV) that recovers after several minutes. *B*: in a recording from a dLGN interneuron, SNAP (500 μM) did not alter the membrane potential. Downward deflections represent membrane responses to 10-pA hyperpolarizing current pulses.

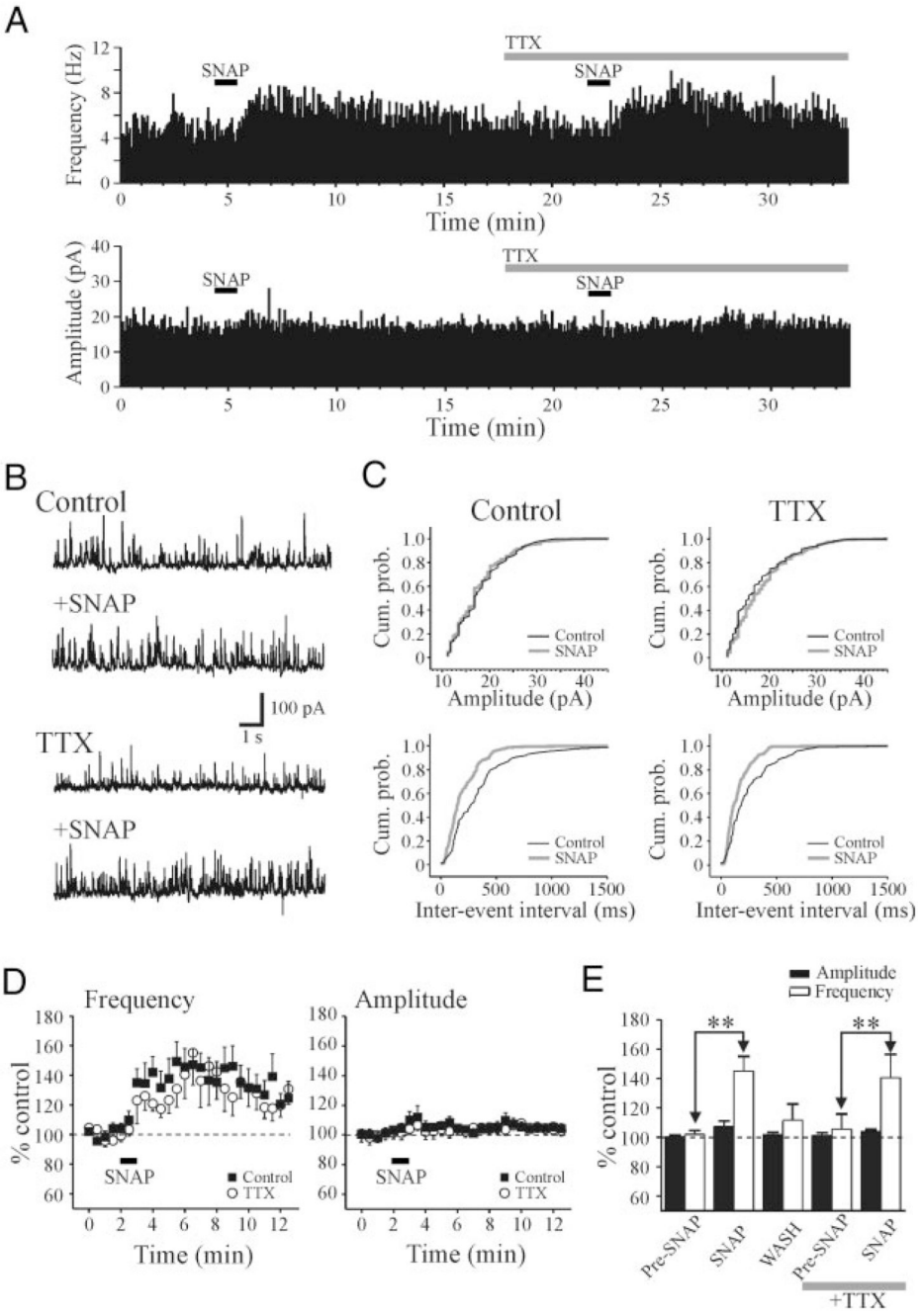

FIG. 3.

SNAP-mediated increase in IPSCs persists in tetrodotoxin (TTX). *A*: histograms illustrating the frequency and amplitude of sIPSCs from a dLGN relay neuron. Histograms were constructed using 5-s bins. In control conditions, SNAP (500 μM) produced a robust increase in sIPSC frequency. In TTX (0.5 μM), the SNAP-mediated increase in sIPSC activity persists. *B*: representative traces from neuron in *A* that illustrate sIPSC activity in different experimental conditions. *C*: cumulative probability plots of amplitude and interevent intervals from neuron in *A*. Note that the clear increase in the interevent intervals even in both control and TTX conditions. *D*: summary plots of the population data ($n = 10$ cells) illustrating the action of SNAP on sIPSC amplitude and frequency. Data are presented

as percentage of control levels in normal ACSF (filled squares) and after TTX (open circles). *E*: histogram plot illustrates the peak SNAP-mediated actions on sIPSC amplitude (filled bars) and frequency (open bars). $^{**}P < 0.01$.

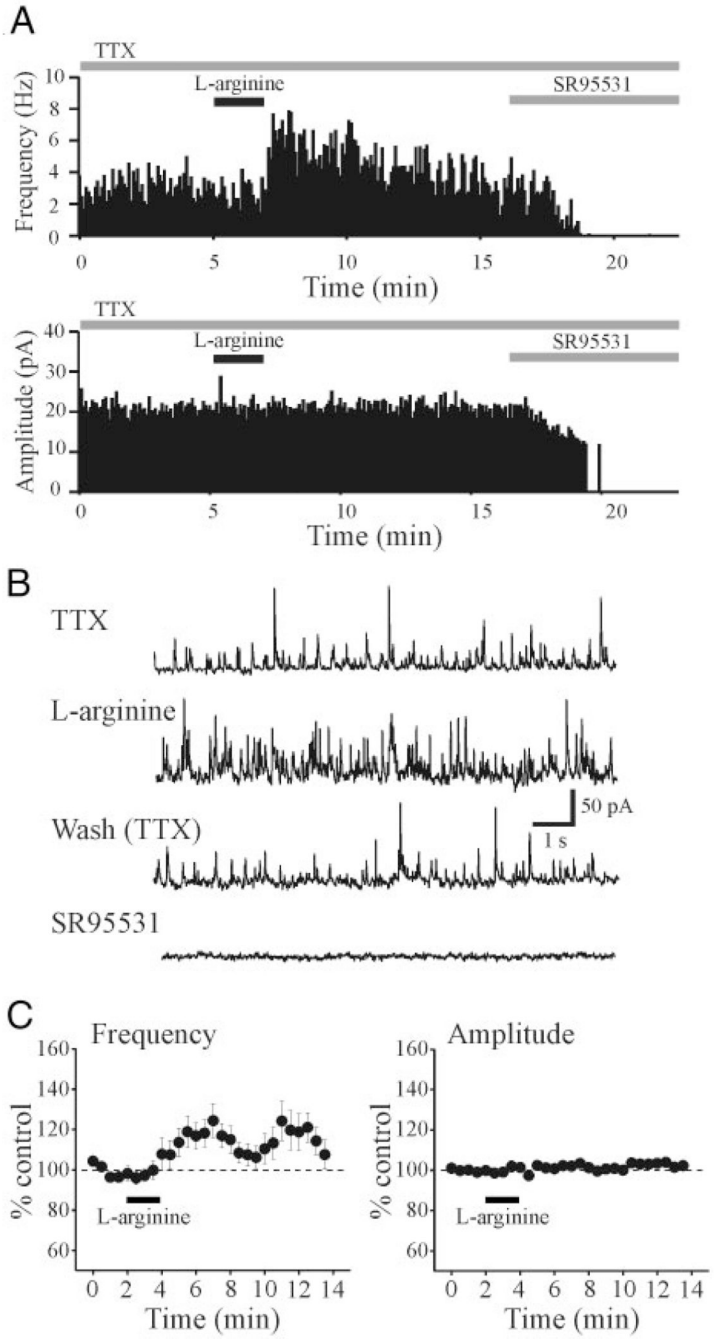

FIG. 4.

L-Arginine increases sIPSC frequency. *A*: histograms illustrating sIPSC frequency and amplitude from a dLGN relay neuron and the response to L-arginine (1 mM, 2 min). TTX (0.5 μM) was present throughout the recording. *B*: representative traces of a voltage-clamp recording shown at a faster time base to illustrate the sIPSCs. Traces illustrate sIPSC activity before and after L-arginine application, wash, and in SR95531 (10 μM). *C*: population data illustrating the effect of L-arginine on sIPSC amplitude and frequency (n = 24 neurons).

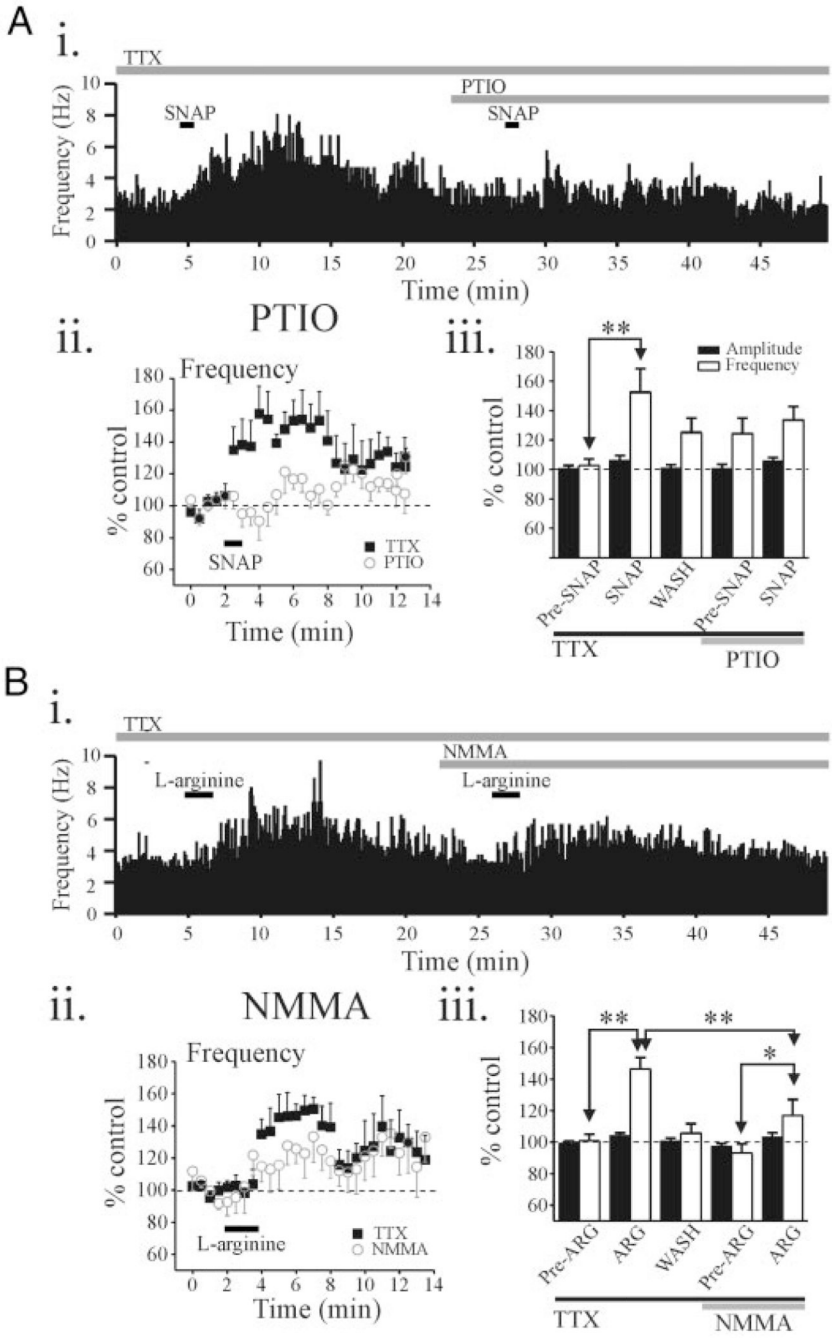

FIG. 5.

sIPSCs induced by SNAP and L-arginine are attenuated by the nitric oxide (NO) scavenger, 2-(4-carboxyphenyl)-4,4,5,5-tetramethylinmidazoline-1-oxide (PTIO), and nitric oxide synthase (NOS) inhibitor N^G-monomethyl-L-arginine acetate (L-NMMA), respectively. *Ai*: histogram illustrating sIPSC frequency over the time course of the experiment. Entire experiment was conducted in the presence of TTX (0.5 μM). *Aii*: population data illustrating SNAP-mediated actions on sIPSC frequency before and in the presence of the PTIO (20 μM, $n = 7$ neurons). Plots illustrate the effect of SNAP on sIPSC frequency in the presence of TTX (filled squares). After recovery, the slice was exposed to PTIO + TTX, and then SNAP was reapplied (open circles). *Aiii*: histogram illustrates population data on peak effect

of SNAP on sIPSC amplitude (filled bars) and frequency (open bars) in different conditions. *Bi*: histogram illustrating sIPSC frequency over the time course of the experiment in an individual dLGN relay neuron. Entire experiment was conducted in the presence of TTX (0.5 μM). *Bii*: population data illustrating L-arginine-mediated actions on sIPSC frequency before and in the presence of the NMMA (100 μM, $n = 6$ neurons). Plots illustrate L-arginine–mediated actions on sIPSC frequency in TTX (filled squares) and after exposure to NMMA + TTX (open circles). *Biii*: histogram illustrates population data on peak effect of L-arginine on sIPSC amplitude (filled bars) and frequency (open bars) in different conditions. $^{**}P < 0.01$, $^{*}P < 0.05$.

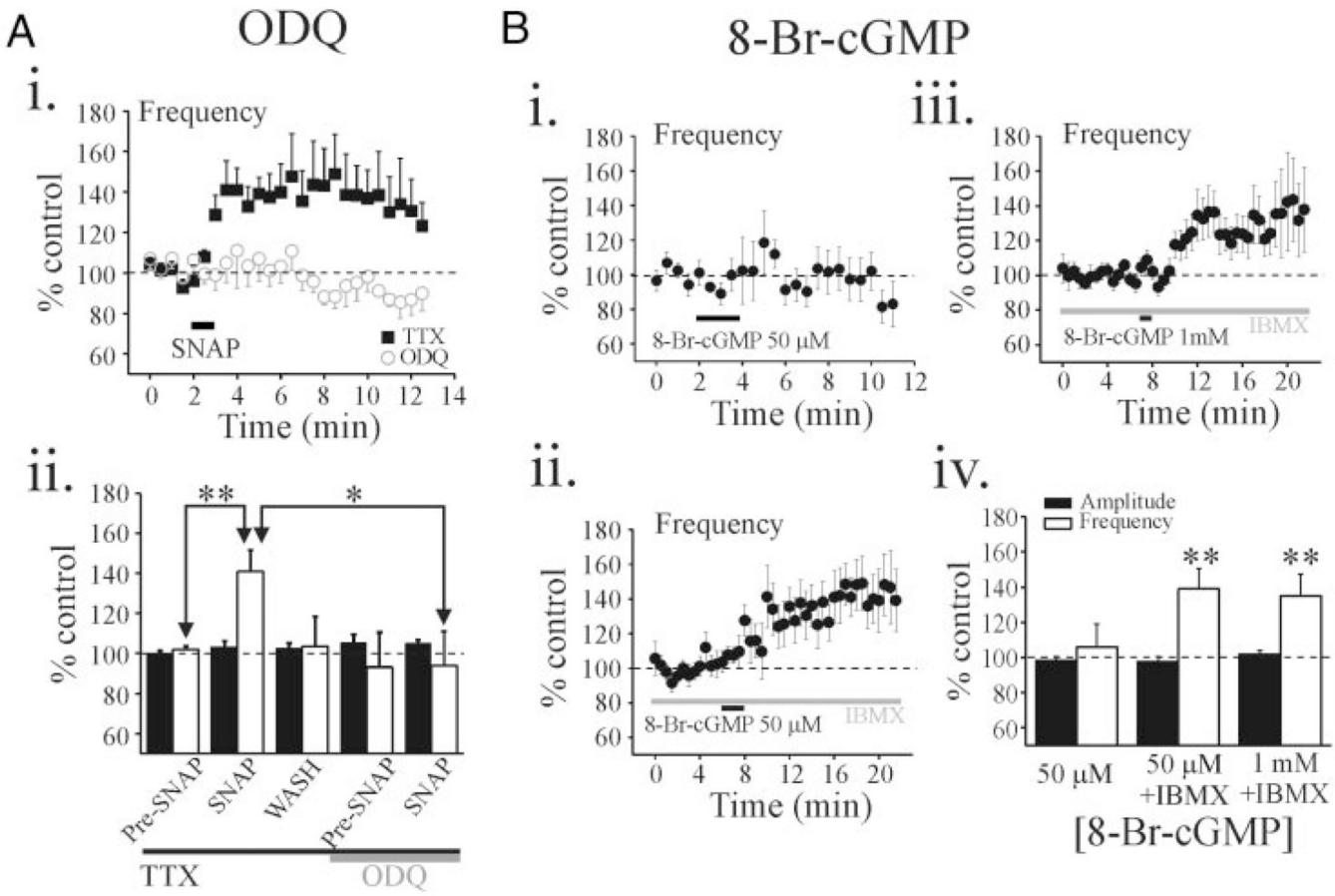

FIG. 6.

SNAP-mediated potentiation is mediated by cGMP-dependent mechanism. *Ai*: population data (n = 7 neurons) illustrating SNAP-mediated actions on sIPSC frequency before and in the presence of the 1*H*-[1,2,4]-oxadiazolo[4,3-a]quinoxalin-1-one (ODQ, 100 µM). Plots illustrate the time course of SNAP-mediated actions on sIPSC frequency in the presence of 0.5 µM TTX (filled squares) and after exposure to ODQ + TTX (open circles). *Aii*: histogram illustrates population data regarding peak effect of SNAP on sIPSC amplitude (filled bars) and frequency (open bars) in different experimental conditions. *B*: population data showing the effect of 8-Br-cGMP on sIPSC activity in normal solution (*Bi*: n = 5 cells) and in the presence of 3-isobutyl-1-methylxanthine (IBMX, 1 mM; *Bii*: n = 8 neurons, *Biii*:n = 13 neurons). All of these experiments were conducted in the presence of TTX (0.5 µM). Note the 2 different 8-Br-cGMP concentrations, 50 µM and 1 mM, illustrated in *Bii* and *Biii*, respectively. *Biv*: histogram illustrates population data regarding peak effect of SNAP on sIPSC amplitude (filled bars) and frequency (open bars) in different experimental conditions. $^{**}P < 0.01$.

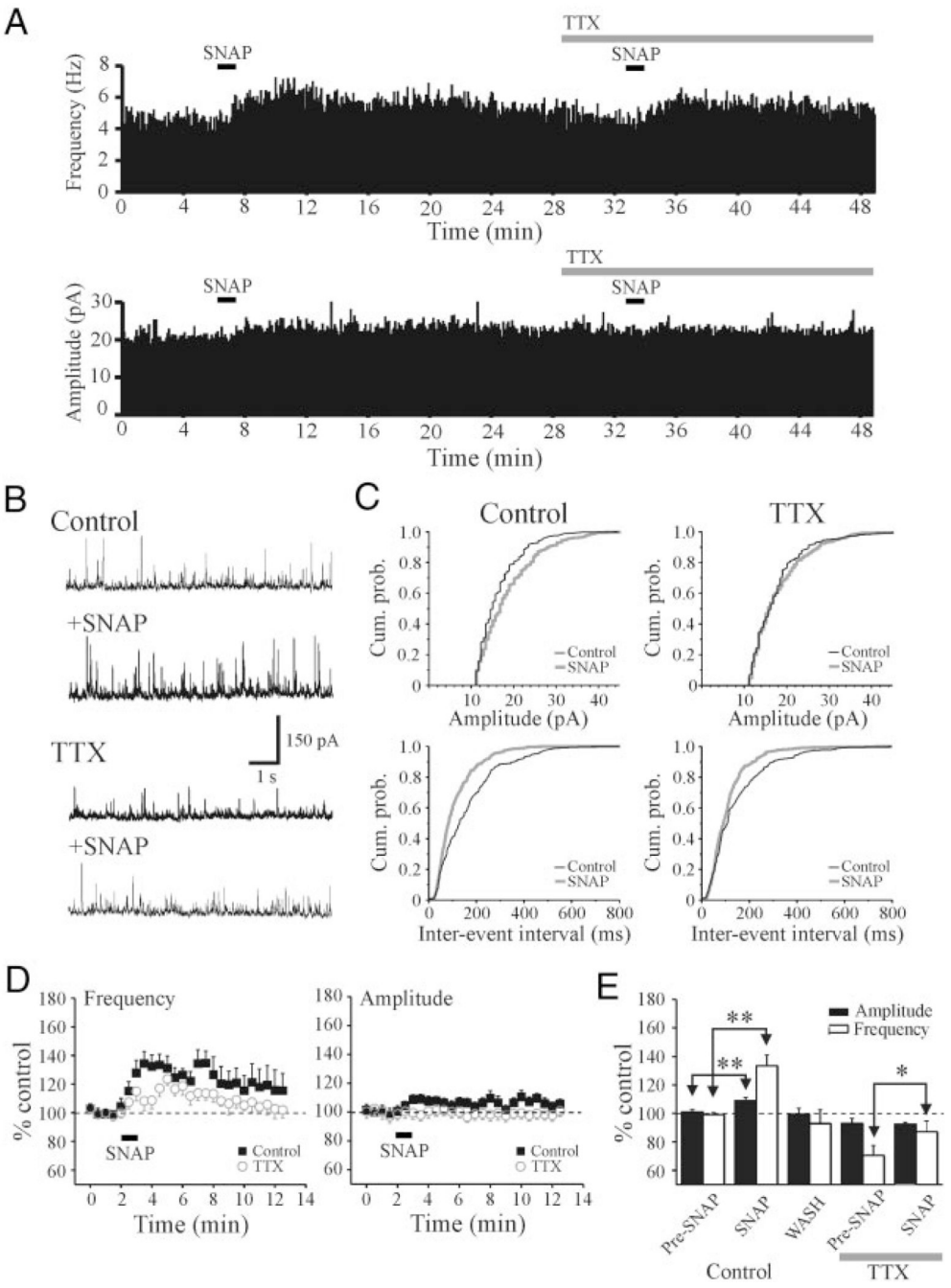

FIG. 7.

SNAP-mediated potentiation of sIPSCs in ventrobasal thalamic (VB) nucleus. *A*: histograms illustrate sIPSC frequency and amplitude from a representative VB relay neuron. In control conditions, SNAP (500 μM) produces an increase in sIPSC activity similar to that observed in dLGN relay neurons. In TTX (0.5 μM), the SNAP-mediated facilitation of sIPSC persists. *B*: representative traces illustrating sIPSC activity in the different experimental conditions. *C*: cumulative probability plots of sIPSC amplitudes and inter-event intervals from neuron in *A*. Note that clear increase in sIPSC amplitudes and interevent intervals produced by SNAP in control conditions. In TTX, SNAP produces an increase only in sIPSC interevent intervals. *D*: population data (n = 9 neurons) indicate an increase in sIPSC frequency by

SNAP before (filled squares) and after TTX application (open circles). *E*: histogram plot illustrates the average peak change in sIPSC amplitude (filled bars) and frequency (open bars) produced by SNAP in different conditions. $^{**}P < 0.01$, $^{*}P < 0.05$.